Formation of laser-induced periodic surface structures during femtosecond laser ablation of highly oriented pyrolytic graphite (HOPG)

Article *in* Lasers in Engineering · January 2013

CITATIONS
2

READS
161

7 authors, including:

Wolke Zhang
China University of Petroleum - Beijing
642 PUBLICATIONS **5,516** CITATIONS
SEE PROFILE

George Amoako
University of Cape Coast
31 PUBLICATIONS **89** CITATIONS
SEE PROFILE

Jielan Li
Tianjin Medical University Cancer Institute and Hospital
739 PUBLICATIONS **2,609** CITATIONS
SEE PROFILE

Lasers in Eng., Vol. 25, pp. 397–404
Reprints available directly from the publisher
Photocopying permitted by license only

Formation of Laser-induced Periodic Surface Structures During Femtosecond Laser Ablation of Highly Oriented Pyrolytic Graphite (HOPG)

W. ZHANG[1], M. ZHOU[1,*], G. AMOAKO[1,2], Y-L. SHAO[1], B-J. LI[1], J. LI[1] AND C-Y. GAO[1]

[1]*Centre for Photon Manufacturing Science and Technology, Jiangsu University, Zhenjiang 212013, Jiangsu, China*
[2]*School of Physical Science, University of Cape Coast, Cape Coast, Ghana*

Formation of laser-induced periodic surface structures (LIPSS) during femtosecond laser ablation of highly oriented pyrolytic graphite (HOPG) is investigated. Using a 1 kHz femtosecond pulses (pulse width 130 fs, centre wavelength 800 nm) for micro-processing on HOPG, the calculated ablation threshold is 0.19 J/cm^2. Two kinds of different periodic nanostructures were seen through scanning electron microscopy (SEM) characterization of the ablated material surface. These were low-spatial-frequency structures with period of about 400 nm and high-spatial-frequency structures with period of about 100 nm. Formation conditions of the nanostructures are analysed by changing the parameters such as laser energy and pulse number. This result would make femtosecond laser direct-write technologies of carbon nanostructures possible.

Keywords: Femtosecond laser, ablation, laser-induced periodic surface structures (LIPSS), highly oriented pyrolytic graphite (HOPG), high-spatial-frequency LIPSS (HSFL), low-spatial-frequency LIPSS (LSFL), carbon nanostructures

1. INTRODUCTION

During ultra-short laser micro-machining of materials, laser-induced periodic surface structures (LIPSS) may be observed in the multi-pulse ablated craters

*Corresponding author: Tel: +86 511 8879 1458; Fax: +86 511 8879 1288; E-mail: zm_laser@126.com

or ditches, such as the "ripple". It was first proposed by Birnbaum [1] in the experimental interactions between laser radiation and semiconductors. Since then, LIPSS have been reported on virtually all materials [2-11], including metals, dielectrics and polymers, while the laser could be either pulsed or continuous wave (CW).

Sipe *et al* [12] proposed a theory which considered that the interaction of an electromagnetic wave with a microscopically rough surface could generate the periodic surface structures like interference fringes, with configurations dependent on wavelength, pulse width, polarization of laser beam and surface conditions of materials. Subsequently, Borowiec and Haugen [13] reported the formation of sub-wavelength sized ripples for the irradiation of various compound semiconductors, including InP by 50 to 130 fs laser pulses at several wavelengths (800, 1300, and 2100 nm) and typically between 1 and 100 pulses per spot. Near the ablation threshold, they reported the formation of high-spatial-frequency LIPSS (HSFL), with lateral periods 4.2 to 5.1 times smaller than the wavelength of the incident light, and low-spatial-frequency LIPSS (LSFL), with a spatial period close to the wavelength of the excitation pulse.

Recently, ultrafast pulsed laser ablation of highly oriented pyrolytic graphite (HOPG) is widely used to prepare for a variety of nanostructures, such as deep-subwavelength gratings [14], sharp ridges and wide wings with a poorer aspect ratio [15]. These results give useful information about the deformation process of the solid surface after femtosecond laser irradiation, and may open possibilities for precise control of spontaneous nano-structuring induced by ultrafast laser irradiation.

Here, when using femtosecond laser to perform experiments on HOPG, we found a periodic surface structure composed of subwavelength gratings, with a diameter of about one hundred nanometres and a length ranging from several hundred nanometres to a few microns. Our findings may provide a new method of preparation of carbon nanostructures using femtosecond laser. We therefore, conducted further experiments to study this phenomenon by continuous adjustment and optimization of experimental conditions.

2. EXPERIMENTAL PROCEDURES

Figure 1 shows a schematic diagram of the experimental set-up. Irradiation was carried out using the femtosecond laser (Integra-C-2.5; Quantronix Corporation) with a central wavelength $\lambda = 800$ nm and pulse duration $t_p = 130$ fs. The spatial profile of the beam was nearly Gaussian. The laser was run at a repetition rate of $f = 1$ kHz and single pulse energy could be adjusted from 2 to 200 μJ, while the pulse numbers can be controlled accurately by a time-delay device (DG535; Stanford Research Systems, Inc.).

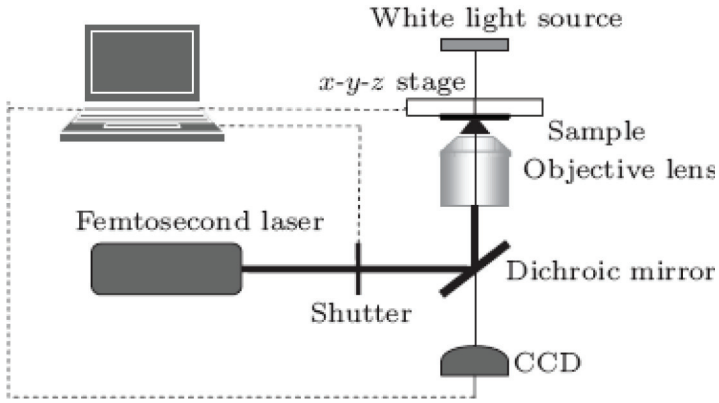

FIGURE 1
Schematic diagram of the experimental set-up.

Samples used in experiments were HOPG, which were placed at a three-dimensional motorized stage and the action of shutter (GC3-003001; China Daheng Group, Inc.) simultaneously. The laser beam was focused to a spot size of around 4 μm and 2. 5 μm by means of a microscope objective lenses (10× and 20× with numerical apertures 0.3 and 0.4, respectively) on to the surface of the HOPG sample. The laser beam was linearly polarized light, and irradiated perpendicularly to the sample.

To examine the topography of the HOPG samples after laser treatment they were analysed using an atomic force microscope (AFM) (AA2000; Angstrom Advanced, Inc.) and a scanning electron microscope (SEM) (JSM-7001F; JEOL, Ltd.)

3. RESULTS AND DISCUSSION

At first, samples were irradiated by single pulses at 10 to 100 μJ. AFM measurement of each ablation crater indicates that when energy is less than 40 μJ, ablation depth increases with laser energy rapidly, at 40 to 70 μJ the ablation depth does not change significantly, and the recurrence of a faster increase was seen with a depth of above 200 nm with the energy increasing from 80 to 100 μJ.

Ablation spot size was measured using SEM images of the ablated material. Using the spatial distribution of the laser beam, the fluence can be calculated by the integral of a single pulse [16]:

$$E=\frac{2U}{\pi\omega_0^2}\exp\left(-\frac{2r^2}{\omega_0^2}\right) \tag{1}$$

where U is pulse energy and ω_0 is beam waist radius. Equation (1) can be transformed to give

$$S = 0.5\pi\omega_0^2 \ln\left(\frac{\phi_0}{\phi_{th}}\right) \tag{2}$$

where ϕ_0 is peak power, ϕ_{th} is threshold of the material and S is ablation area.

Because of the linear relationship between ablation spot size and logarithmic light intensity, waist radius was calculated using the slope of the line (see Figure 2), and the intercept on the horizontal axis (see Figure 3) was used to calculate the ablation threshold ϕ_{th}. Using Equation (2), ϕ_{th} is 0.19J/cm^2, which is close to the theoretical value of 0.185 J/cm^2 [17].

For single pulse ablation, just shallower ablation traces instead of LSFL or HSFL were generated with the energy increased from 2 to 200 μJ. However, during multi-pulse ablation experiments, at the energy of 2 μJ (see Figure 4(a)), LSFL appears after ablation with 5 pulses. The LSFL was located at the centre of the spot and covering 1/4 of the area of the whole spot; further, when the pulse number increased to 50, besides LSFL still covering 1/4 of the area of the whole spot, a few HSFL were present at the edge of the crater. The crater depth increased with further increase of the pulse number, which increased the area of HSFL slightly. In addition, while the energy increases to 8 μJ (see Figure 4(b)), the structure does not change significantly, only the area of both LSFL and HSFL increased to 80% of the total area of the spot. After ablation by 500 pulses, the craters have a depth of several microns, and there could be found LSFL still existing at the bot-

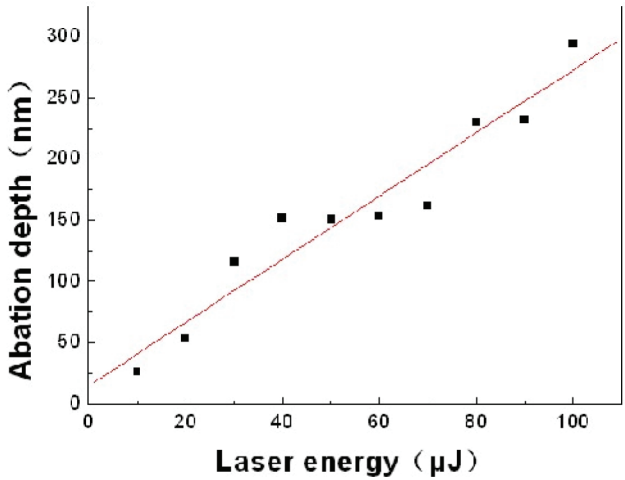

FIGURE 2
Relationship between laser energy and ablation depth.

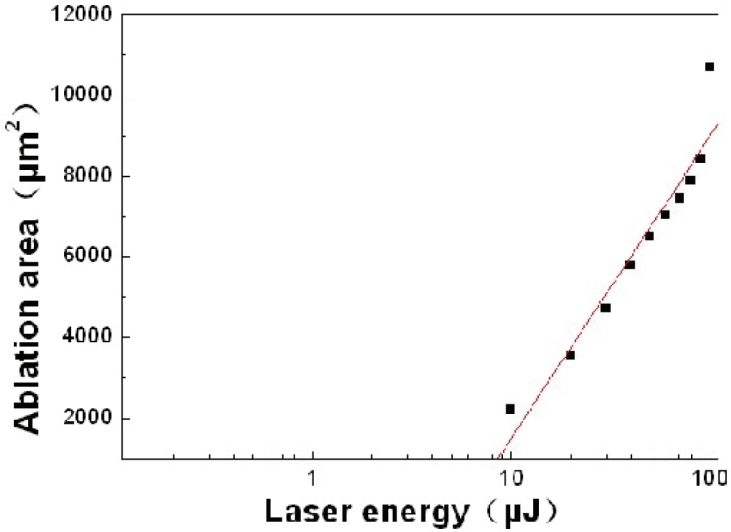

FIGURE 3
Relationship between laser energy and ablation area.

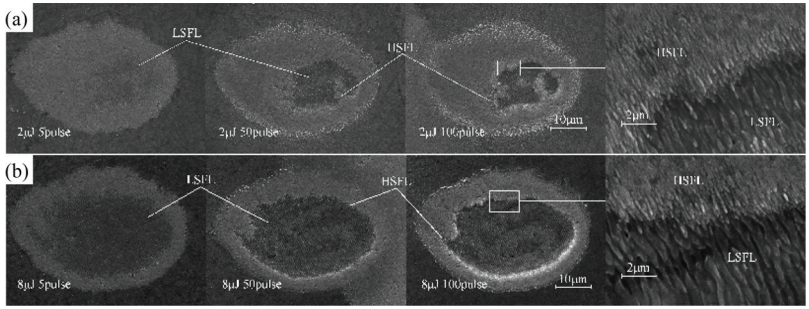

FIGURE 4
SEM images of ablation craters at laser energies of (a) 2 μJ and (b) 8 μJ.

tom of the craters while HSFL were only present at the slopes. When the energy was increased up to 100 μJ, all the periodic structures disappeared, and the entire spot craters merged into a deep crater.

We also studied and compared the characteristics of periodic structures at different laser pulse energies. For HSFL (see Figure 5), the period of the structure increased with the energy. Figure 5 shows the stripe structures formed at 50, 100, 200 μJ by line scan, with the periods increasing gradually from about 100 nm to about 150 nm, and finally to about 200 nm. It was seen that the stripe structure was also significantly shorter in length, while the value decreased to a few hundred nanometres at 200 μJ, and it changed to

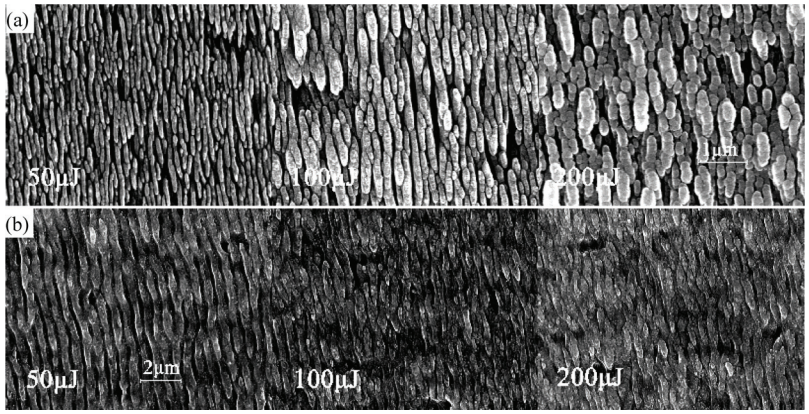

FIGURE 5
SEM micrographs of (a) HSFL and (b) LSFL at different laser energies: 50, 100 and 200 μJ.

small stick or ball at some places. As one can see from Figure 5, for LSFL the stripe width had no significant change, but it is obvious that the ripples become shorter and overlap with each other.

Presently, there are many interpretations for the forming of these periodic streaks; these include the properties of the laser beam, the freezing of surface acoustic waves, and the plasma concentration. Whatever the interpretation is, most of the patterns are similar, and seem to be nearly independent of the material properties and the periodic gratings structure is obtained by a linearly polarized incident laser. The formation mechanism of this kind of ripples is usually based upon the interference between incident light and generated plasma. The stripe period d can be calculated using [18]

$$d = \frac{\lambda}{(n \pm \sin\theta)} \tag{3}$$

where λ is the wavelength of incident light, θ is the angle of incident laser and n denotes the material refractive index. This relationship indicates that the period can be changed by altering the wavelength, incident angle or the refractive index. In our work it was found that the period of LSFL is about 400 nm. Here, the refractive index of HOPG is around 1.93 to 2.07, the incident angle is 0º when the laser irradiates perpendicularly, and the laser wavelength is 800 nm. Using these parameters the result given by Equation (3) is about 400 nm, which is consistent with the experimental measurement. Equation (3) is obviously inapplicable to the situation in which the period of LSFL is about 100 nm. Bonse *et al* [19] employed the generation of second-harmonic generation (SHG) to explain the formation of HSFL. They proposed

that the initial HSFL would roughen the material surface which might increase the probability of SHG greatly. In this situation, the period is described as

$$d = \frac{\lambda}{2n} \tag{4}$$

With the relevant parameters, the period is about 200 nm, which is larger than the result obtained in the low-energy experiment, but is consistent with the period of 200 μJ experiment.

4. CONCLUSIONS

The results indicate that we can get two types of periodic structures by multi-pulse ablation processing: high-spatial-frequency LIPSS (HSFL) and low-spatial-frequency LIPSS (LSFL), with the latter having a larger period. The configurations of our carbon nanostructures are similar to typical periodic surface structures though there are some differences in detail. The formation mechanism and the specific structure require further investigation. We also observed that there are no periodic nanostructures formed on the surface of highly oriented pyrolytic graphite (HOPG) after high-energy ablation by a single laser pulse. However, for the same structures, the required quantity of high-energy laser pulse is less than the low-energy. And we believe that our discovery may play a very important role in the development of future large-scale carbon nano-structured direct-write technology.

ACKNOWLEDGEMENTS

This work was supported by the Jiangsu Natural Science Foundation under Grant CX10B_258Z, the China Postdoctoral Science Foundation funded project (20100481093), the National Natural Science Foundation of China under Grant 50975129 and the A Project Funded by the Priority Academic Program Development of Jiangsu Higher Education Institutions (PAPD).

REFERENCES

[1] Birnbaum M. Semiconductor surface damage produced by ruby lasers. *Journal of Applied Physics* **36**(11) (1965), 3688–3689.

[2] van Driel H.M., Sipe J.E. and Young J.F. Laser-induced periodic surface structure on solids: A universal phenomenon. *Physics Review Letters* **49**(26) (1982), 1955–1958.

[3] Guosheng Z., Fauchet P.M. and Siegman A.E. Growth of spontaneous periodic surface structures on solids during laser illumination. *Physics Review B: Condensed Matter and Materials Physics* **26**(10) (1982), 5366–5381.

[4] Young J.F., Sipe J.E. and van Driel H.M. Laser-induced periodic surface structure. III. Fluence regimes, the role of feedback, and details of the induced topography in germanium. *Physics Review B: Condensed Matter and Materials Physics* **30**(4) (1984), 2001–2015.

[5] Temple P.A. and Soileau M.J. Polarization charge model for laser-induced ripple patterns in dielectric materials. *IEEE Journal of Quantum Electronics* **17**(10) (1981), 2067–2072.

[6] Siegman A.E. and Fauchet P.M. Stimulated Wood's anomalies on laser illuminated surfaces. *IEEE Journal of Quantum Electronics* **22**(8) (1986), 1384–1403.

[7] Young J.F., Sipe J.E. and van Driel H.M. Regimes of laser-induced periodic surface structure on germanium: radiation remnants and surface plasmons. *Optics Letters* **8**(8)(1983), 431–433.

[8] Preston J.S., van Driel H.M. and Sipe J.E. Pattern formation during laser melting of silicon. *Physics Review B: Condensed Matter and Materials Physics* **40**(3)(1989), 3942–3954.

[9] Ashkenasi D., Rosenfeld A., Varel H., Wahmer M. and Campbell E.E.B. Laser processing of sapphire with picosecond and sub-picosecond pulses. *Applied Surface Science* **120**(1-2) (1997), 65-80.

[10] Dumitru G., Romano V., Weber H.P., Sentis M. and Marine W. Femtosecond ablation of ultrahard materials. *Applied Physics A: Materials Science Processing* **74**(6) (2002), 729–739.

[11] Yu J.J. and Lu Y.F. Laser-induced ripple structures on Ni-P substrates. *Applied Surface Science* **148**(3-4) (1999), 248–252.

[12] Sipe J.E., Young J.F., Preston J.S. and van Driel H.M. Laser-induced periodic surface structure. I. Theory. *Physics Review B: Condensed Matter and Materials Physics* **27**(2) (1983), 1141–1154.

[13] Borowiec A. and Haugen H. K. Subwavelength ripple formation on the surfaces of compound semiconductors irradiated with femtosecond laser pulses. *Applied Physics Letters* **82**(25) (2003), 4462–4464.

[14] Huang M., Zhao F-L., Cheng Y., Xu N-S. and Xu Z-Z. Mechanisms of ultrafast laser-induced deep-subwavelength gratings on graphite and diamond. *Physics Review B: Condensed Matter and Materials Physics* **79**(12) (2009), 125436.

[15] Tomita T., Kumai R., Matsuo S., Hashimoto S. and Yamaguchi M. Cross-sectional morphological profiles of ripples on Si, SiC, and HOPG. *Applied Physics A: Materials Science Processing* **97**(2) (2009), 271–276.

[16] Liu J.M. Simple technique for measurements of pulsed Gaussian-beam spot sizes. *Optics. Letters* **7**(5) (1982), 196–198.

[17] Jeschke H.O., Garcia M.E. and Bennemann K.H. Theory for the ultrafast ablation of graphite films. *Physics Review Letters* **87**(1) (2001), 015003.

[18] Bonch-Bruevich A.M., Libenson M.N., Makin V.S. and Trubaev V.V. Surface electromagnetic waves in optics. *Optical Engineering* **31**(4) (1992), 718–730.

[19] Bonse J., Munz M. and Sturm H. Structure formation on the surface of indium phosphide irradiated by femtosecond laser pulses. *Journal of Applied Physics* **97**(1) (2005), 013538.